AFRL-ML-WP-TP-2006-480

PRECIPITATION COATING OF MONAZITE ON WOVEN CERAMIC FIBERS: I. FEASIBILITY (POSTPRINT)

Geoff E. Fair, Randall S. Hay, and Emmanuel E. Boakye

JULY 2006

STINFO COPY

MATERIALS AND MANUFACTURING DIRECTORATE
AIR FORCE RESEARCH LABORATORY
AIR FORCE MATERIEL COMMAND
WRIGHT-PATTERSON AIR FORCE BASE, OH 45433-7750

REPORT DOCUMENTATION PAGE					*Form Approved* *OMB No. 0704-0188*

The public reporting burden for this collection of information is estimated to average 1 hour per response, including the time for reviewing instructions, searching existing data sources, searching existing data sources, gathering and maintaining the data needed, and completing and reviewing the collection of information. Send comments regarding this burden estimate or any other aspect of this collection of information, including suggestions for reducing this burden, to Department of Defense, Washington Headquarters Services, Directorate for Information Operations and Reports (0704-0188), 1215 Jefferson Davis Highway, Suite 1204, Arlington, VA 22202-4302. Respondents should be aware that notwithstanding any other provision of law, no person shall be subject to any penalty for failing to comply with a collection of information if it does not display a currently valid OMB control number. **PLEASE DO NOT RETURN YOUR FORM TO THE ABOVE ADDRESS**.

1. **REPORT DATE** *(DD-MM-YY)* July 2006	2. **REPORT TYPE** Journal Article Postprint	3. **DATES COVERED** *(From - To)*

4. **TITLE AND SUBTITLE** PRECIPITATION COATING OF MONAZITE ON WOVEN CERAMIC FIBERS: I. FEASIBILITY (POSTPRINT)	5a. **CONTRACT NUMBER** In-house
	5b. **GRANT NUMBER**
	5c. **PROGRAM ELEMENT NUMBER** N/A
6. **AUTHOR(S)** Geoff E. Fair and Randall S. Hay (AFRL/MLLN) Emmanuel E. Boakye (UES Inc.)	5d. **PROJECT NUMBER** N/A
	5e. **TASK NUMBER** N/A
	5f. **WORK UNIT NUMBER** N/A

7. **PERFORMING ORGANIZATION NAME(S) AND ADDRESS(ES)** Ceramics Branch (AFRL/MLLN) Metals, Ceramics, & NDE Division Materials and Manufacturing Directorate Air Force Research Laboratory, Air Force Materiel Command Wright-Patterson Air Force Base, OH 45433-7750	UES Inc. 4401 Dayton-Xenia Rd. Dayton, OH 45432	8. **PERFORMING ORGANIZATION REPORT NUMBER** AFRL-ML-WP-TP-2006-480

9. **SPONSORING/MONITORING AGENCY NAME(S) AND ADDRESS(ES)** Materials and Manufacturing Directorate Air Force Research Laboratory Air Force Materiel Command Wright-Patterson AFB, OH 45433-7750	10. **SPONSORING/MONITORING AGENCY ACRONYM(S)** AFRL-ML-WP
	11. **SPONSORING/MONITORING AGENCY REPORT NUMBER(S)** AFRL-ML-WP-TP-2006-480

12. **DISTRIBUTION/AVAILABILITY STATEMENT**
Approved for public release; distribution is unlimited.

13. **SUPPLEMENTARY NOTES**
© 2006 The American Ceramic Society. The U.S. Government is joint author of the work and has the right to use, modify, reproduce, release, perform, display, or disclose the work.
Journal article published in the Journal of the American Ceramic Society, Vol. 90, No. 2 (2007).
PAO Case Number: AFRL/WS 06-1929, 08 Aug 2006. Paper contains color.

14. **ABSTRACT**

Monazite coatings were deposited on woven cloths and tows of Nextel^{TM} 610 fibers by heterogeneous nucleation and growth using solution precursors. Initial experiments revealed two coating regimes in which monazite was either precipitated both in solution and onto the fiber surfaces or only onto the fiber surfaces depending on the precursor solution concentration and fiber surface area. In both cases, regions of tightly packed fibers within cloths were uncoated. Image analysis of coated fiber cross-sections revealed a strong correlation between fiber separation and coating thickness, suggesting that coating of tightly packed fibers was limited by transport of the reactants in solution to these areas.

15. **SUBJECT TERMS**

16. **SECURITY CLASSIFICATION OF:**			17. **LIMITATION OF ABSTRACT:** SAR	18. **NUMBER OF PAGES** 14	19a. **NAME OF RESPONSIBLE PERSON** (Monitor) Geoff E. Fair
a. **REPORT** Unclassified	b. **ABSTRACT** Unclassified	c. **THIS PAGE** Unclassified			19b. **TELEPHONE NUMBER** *(Include Area Code)* N/A

Standard Form 298 (Rev. 8-98)
Prescribed by ANSI Std. Z39-18

journal _____

Precipitation Coating of Monazite on Woven Ceramic Fibers: I. Feasibility

Geoff E. Fair[†] and Randall S. Hay

Materials and Manufacturing Directorate, Air Force Research Laboratory, Wright-Patterson AFB, Ohio 45433

Emmanuel E. Boakye

UES Inc., Dayton, Ohio 45432

Monazite coatings were deposited on woven cloths and tows of Nextel™ 610 fibers by heterogeneous nucleation and growth using solution precursors. Initial experiments revealed two coating regimes in which monazite was either precipitated both in solution and onto the fiber surfaces or only onto the fiber surfaces depending on the precursor solution concentration and fiber surface area. In both cases, regions of tightly packed fibers within cloth were uncoated. Image analysis of coated fiber cross sections revealed a strong correlation between fiber separation and coating thickness, suggesting that the coating of tightly packed fibers was limited by transport of the reactants in solution to these areas. By adopting a coating procedure in which the tightly packed regions are saturated with reactants before precipitation, more uniform coatings of monazite were obtained throughout the cloth; however, the strength of as-coated and heat-treated fibers was degraded and remains problematic.

I. Introduction

To realize the benefits of fiber reinforcement in ceramic matrix composites (CMCs), the matrix must transfer loads to the fibers but decouple from the fibers during fracture so that the fibers remain intact and continue to bear loads.[1–4] Functional fiber coatings such as carbon and boron nitride enhance the decoupling and load transfer capabilities of CMCs but are inherently susceptible to oxidation in the high-temperature, oxygen, and water-containing environments for which such materials are being considered (hot section turbine engine components, etc., for which temperatures in excess of 1000°C are expected).[5,6] Recent work has focused on the development of oxidation resistant analogues of C and BN.[7,8] Monazite (LaPO$_4$) and other related oxides have been shown to function as effective fiber coatings in dense matrix CMCs and, as oxides, are not susceptible to the oxidation problems of C and BN.[9]

Various methods have been used to apply oxide coatings to ceramic fibers, including chemical vapor deposition (CVD)[10] and continuous dip coating using solution and sol-derived precursors.[11,12] Coating processes suitable for mixed oxides that are applicable to multi-filament tows are generally not amenable to coating cloths or woven preforms of ceramic fibers. Several techniques based on electrostatic or electrophoretic deposition have been conceived but result in less than optimal coatings.[13–15] Existing methods for coating woven cloths and preforms via CVD are costly, require hazardous chemicals, and are not readily applicable to stoichiometric multi-component oxides.[10] With existing coating technology for oxide fibers, coatings are applied to multi-filament tows that must then be woven to produce cloths and performs.[16] During the weaving of coated fibers, the coatings may be damaged; consequently, a process for the coating of woven fibers is advantageous from the standpoint of avoiding such damage. Similarly, there is an economic benefit to coating woven fibers in that a higher throughput may be achieved in a continuous process. This is important because fiber coating can be a significant fraction of composite cost.

The objective of this work was to develop a simple, low-cost method for the deposition of high-quality, mixed-oxide fiber coatings onto ceramic fiber cloths and woven preforms. Recent work by Yano *et al.*[17] suggests that such a process may be achievable; however, several key issues must be addressed in the development of the coating process: (1) coating of tightly packed fibers located where tows cross over one another in the weave; this issue has been the primary hurdle to the development of dip-coating methods for cloth coating; (2) fiber strength retention during processing; and (3) adherence of the resulting coatings. The coating process should not degrade the strength of the fibers during processing or service as composite properties are optimized by having the highest fiber strength possible; composite strength scales linearly with fiber strength.[1] The coatings must not spall off during subsequent handling in the processing of the composite.

A method for the coating of woven ceramic fibers (2D cloths, 3D preforms, etc.) has been developed in which a LaPO$_4$ coating is applied from solution by heterogeneous nucleation and growth directly on the woven fibers submerged in a precursor solution. The method exploits the temperature and concentration dependence of the reaction between lanthanum citrate and phosphoric acid. The results of early experiments suggested that coating regions of tightly packed fibers were limited by reactant transport. A revised solution-based coating process was developed in which the tightly packed regions were saturated with a high concentration of reactants before precipitation; this modified method for coating woven ceramic fibers resulted in more uniform coating of individual fibers in the tows. Coatings produced using both methods are characterized and the results are compared and discussed.

II. Experimental Procedure

(1) Precursor Solution Preparation

Precursor solutions of phosphoric acid and lanthanum citrate were prepared by dissolving concentrated phosphoric acid (Fisher Scientific Co., Pittsburgh, PA) or a combination of lanthanum nitrate (Aldrich Chemical Co., Milwaukee, WI), and citric acid (Fisher Scientific Co.) in de-ionized water. A range of precursor solution concentrations were investigated. Precursor solution concentrations are expressed in terms of mass of LaPO$_4$ yield per volume of mixed solution assuming a complete reaction, e.g. 5 g LaPO$_4$/L. Initial experiments used precursor concentrations of 1–5 g LaPO$_4$/L. Later experiments, using a

1

revised coating procedure, used solutions prepared to yield 100 g $LaPO_4$/L. The La:citrate ratio of the solutions was either 1:2 or 1:5. The La:P ratio was fixed at 1:1 for all experiments. The lanthanum citrate and phosphoric acid solutions were chilled to $\sim 5^\circ C$ before mixing during the coating procedure.

(2) Coating Procedures

(A) Initial Cloth and Tow Coating Experiments (Process A): Nextel™ 610 aluminum oxide fiber tows and eight harness satin weave cloths (1500 denier, 3M Co., St. Paul, MN) were used for all coating experiments. Initial experiments to coat both cloths and fiber tows were performed using a method to precipitate hydrated $LaPO_4$ (rhabdophane: $LaPO_4 \cdot nH_2O$) developed for producing nanoparticle sols for coating fiber tows.[18] The precursor solutions were first chilled to $\sim 5^\circ C$. The chilled precursors were then added to a stirred vessel containing the fibers to be coated (cloths or tows). The mixed solution was allowed to equilibrate to room temperature and then heated to precipitate $LaPO_4 \cdot nH_2O$. Precipitation typically occurred at 20°–$25^\circ C$, although the solutions were heated to a final temperature of $35^\circ C$ to assure complete precipitation. Equilibration followed by heating to $35^\circ C$ typically took ~ 80 min. The fibers were then removed from the vessel and rinsed for 20 s in 400 mL of de-ionized water to remove any remaining dissolved chemicals and loosely bound solids. The fibers were then dried at $100^\circ C$ and fired for 1 h at $900^\circ C$ in laboratory air to convert $LaPO_4 \cdot nH_2O$ to monazite and bond the coating to the fibers. The entire coating procedure was repeated four or five more times to increase the coating thickness.

In addition, a number of experiments were designed such that the precipitation occurred at a constant temperature (10°, 20° or $40^\circ C$). This was accomplished by adding the chilled precursors (3 g monazite/L, La:citrate = 1:5) to a stirred vessel submerged in an isothermal bath. The temperature of the mixed solution equilibrated to the bath temperature within 5 min. For precipitation at $40^\circ C$, the precursor solutions were warmed to $40^\circ C$ before mixing. The time required to precipitate $LaPO_4 \cdot nH_2O$ was measured at each temperature; precipitation was assumed to be complete when the solution became fully opaque. To examine the coating evolution on the fiber surface, fiber tows were suspended in the reaction vessel and removed from the bath at various time intervals, dried, and fired 1 h at $900^\circ C$ in air.

(B) Revised Cloth Coating Procedure (Process B): A revised coating procedure was adopted to improve coating coverage and uniformity. Coating was performed by submerging cloths previously saturated with a chilled, concentrated precursor solution (100 g monazite/L) into warm water to precipitate the coating onto the fibers. Ten millilitres portions of both chilled precursor solutions (lanthanum citrate and phosphoric acid) prepared to yield 100 g monazite/L were mixed in a large beaker to which a 3in. × 3in. piece of cloth was added. The beaker containing the mixed solutions and cloth was placed in an ultrasonic bath for 15 s. The beaker was removed from the bath and the cloth was removed from the solution. Excess solution was drained from the cloth against the side of the beaker. The cloth, saturated with precursor solution, was submerged in a vessel containing warm de-ionized water at $50^\circ C$ to precipitate $LaPO_4 \cdot nH_2O$ rapidly. After 5 min in the warm water bath, the cloth was removed and rinsed for 20 s in 400 mL of de-ionized water to rinse away any remaining dissolved chemicals and loosely bound solids. The cloth was subsequently dried in air at $100^\circ C$ for 15 min and finally placed in a tube furnace at $900^\circ C$ for 5 min in air. The entire coating procedure was repeated 13 times for a total of 14 coats/cloth.

(3) Characterization

Coatings were characterized using both polished cross-sections of the coated cloths[19,20] and fiber tows extracted from the coated cloths. Cross-sections and surfaces of extracted tows were examined using a scanning electron microscope (SEM) (Leica 360 FE,

Ernst Leitz, Westler, Germany). Phase analysis of the coated cloths was performed using an X-ray diffractometer (Rigaku Rotaflex with Cu$K\alpha$ radiation, Rigaku Co., Tokyo, Japan); transmission electron microscopy (TEM) (Phillips CM200FEG, Eindhoven, the Netherlands) was performed to characterize the coating microstructure and identify any intergranular phases. SEM micrographs of the polished cross-sections were taken at several magnifications and image sizes for image analysis of coating thickness.[21] Mechanical testing of the coated fibers to examine the retained strength was performed on an MTS machine (Synergie 400, MTS Systems Corp., Eden Prairie, MN); tows were extracted from the coated cloths and 50 fibers were tested from each coating condition using a 25.4 mm gauge length.[22,23] Fibers were tested in the as-processed condition; in addition, fibers with uniform coatings produced using the revised cloth coating procedure were tested following a 2-h exposure at $1200^\circ C$ in laboratory air.

III. Results

(1) Initial Cloth and Tow Coating Experiments

Figure 1 schematically illustrates the experimental setup of Process A and shows backscatter SEM micrographs of polished cross-sections of cloths coated five times with precursor solution yielding 4.7 g $LaPO_4$/L. $LaPO_4$ appears white in the micrographs due to average atomic number contrast. The $LaPO_4$ coatings are more uniformly deposited in the regions of loose fiber packing. Where the fibers are tightly packed, i.e. tow crossovers, little or no coating is deposited. The coating around the perimeter of tightly packed tows is quite thick and forms a continuous crust. Fibers extracted from the coated cloth following processing had an average strength of 2.58 ± 0.38 GPa, consistent with values obtained for fibers extracted from desized, uncoated Nextel™ 610 cloths (2.6–2.8 GPa); this indicates that no strength degradation occurred as a result of coating.

Figure 2 shows X-ray diffraction patterns of the coatings from Process A in both the as-processed condition and after heating to $1200^\circ C$ for 5 h in air. $LaPO_4$ and alumina (from the Nextel™ 610 fiber) were the only phases detected. Figure 2 also shows TEM micrographs of the $LaPO_4$ coatings on Nextel™ 610 fibers. The interface between the coating and the fibers was free of any other phases and did not contain trace amorphous $AlPO_4$ as found in some previous coatings.[24]

Figure 3 shows backscatter SEM micrographs of polished cross-sections of loose tows coated five times via Process A with precursor solution yielding 3 g $LaPO_4$/L. In this case, the $LaPO_4$ coating thickness is extremely uniform from fiber to fiber, with little crust formation or fiber bridging. The improved coating uniformity is attributed to the looseness of the fiber tows in the coating solution, which facilitates mass transport of precursor to all fibers equally.

Figure 4 shows coating evolution during a single coating step as a function of time at a constant solution temperature of $20^\circ C$ and a precursor solution concentration of 3 g $LaPO_4$/L. The coating nucleates on the fiber surface within ~ 40 min. The nuclei grow to form an almost continuous coating (60 min), which then grows thicker and begins to crack upon drying and firing (80 and 100 min). Also noted in the figure is the clarity of the precursor solution during the precipitation. Nucleation of the coating on the fiber surface occurs while the solution is still clear. The time necessary to precipitate $LaPO_4 \cdot nH_2O$ via process A for 3 g/L solutions was 360, 100, and 1 min at 10°, 20°, and $40^\circ C$, respectively.

Figure 5 illustrates the effect of both the precursor solution concentration and the fiber loading on the precipitation coating process. High-precursor solution concentration coupled with low fiber loading led to precipitation of $LaPO_4 \cdot nH_2O$ on both the fiber as well as in the bulk solution; in these cases, the coatings were comprised of equiaxed particles and were more prone to crusting and fiber bridging. Low precursor solution concentration coupled with high fiber loading led to growth of the
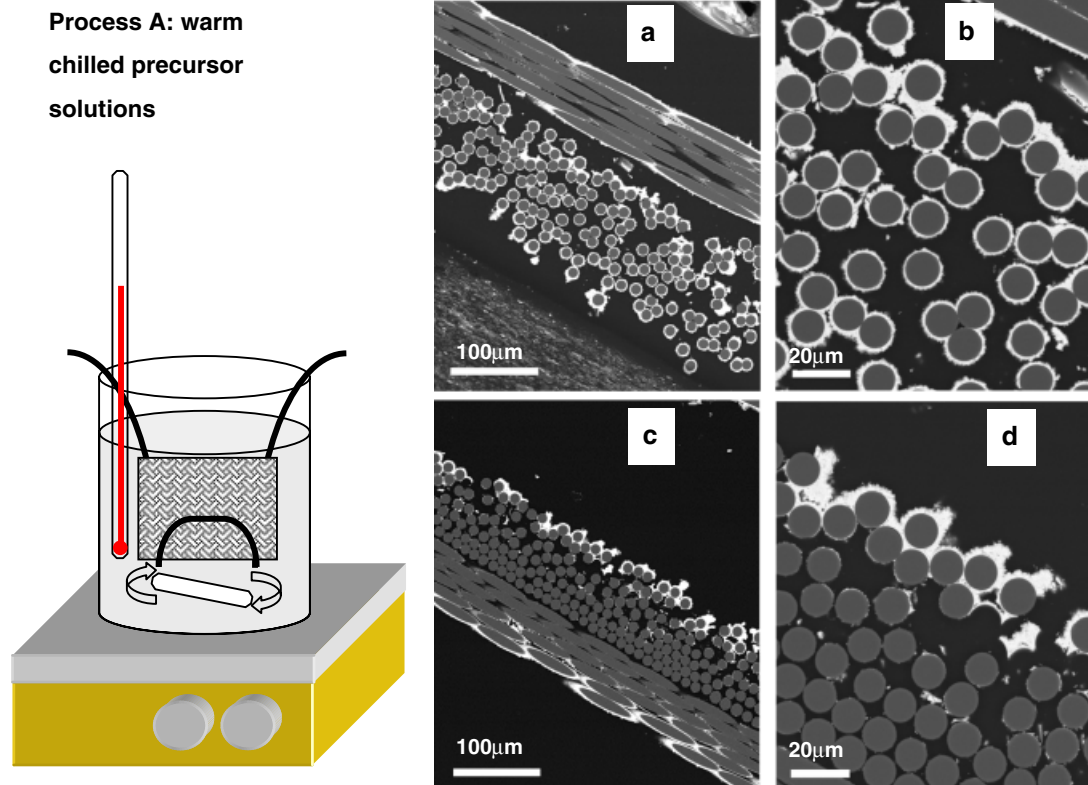
Process A: warm chilled precursor solutions

Fig. 1. Schematic of experimental setup of Process A and backscatter scanning electron microscope micrographs of polished cross-sections of cloths coated five times with precursor solution yielding 4.7 g monazite/L. La:citrate = 1:5. (a) and (b) loosely packed region. (c) and (d) tightly packed region.

coating on the fiber without precipitation in solution, i.e., the precursor solution remained clear during heating to precipitate the coating. In these cases, the coatings were comprised of acicular particles.

Figure 6 shows backscatter SEM micrographs of polished cross-sections of cloths coated six times with precursor solution yielding 1 g LaPO$_4$/L using process A. In this case, the fiber loading was such that no precipitation occurred in solution (upper left-hand corner of Fig. 5). The coatings are uniform in the regions of loosely packed fibers; however, in regions of tight

fiber packing, little or no coating was deposited in the interior of the tow. Minimal fiber bridging was observed.

Figure 7 shows the results of the coating thickness analysis of the SEM micrographs of polished cross-sections of cloths coated six times with precursor solution yielding 1 g LaPO$_4$/L using process A. The average coating thickness of each fiber in the micrographs is plotted as a function of the average fiber separation calculated by assuming the Voronoi polyhedra used in the analysis to be a perfect hexagon.[21] The coating thickness decreases linearly below an average fiber separation of ∼3 μm;

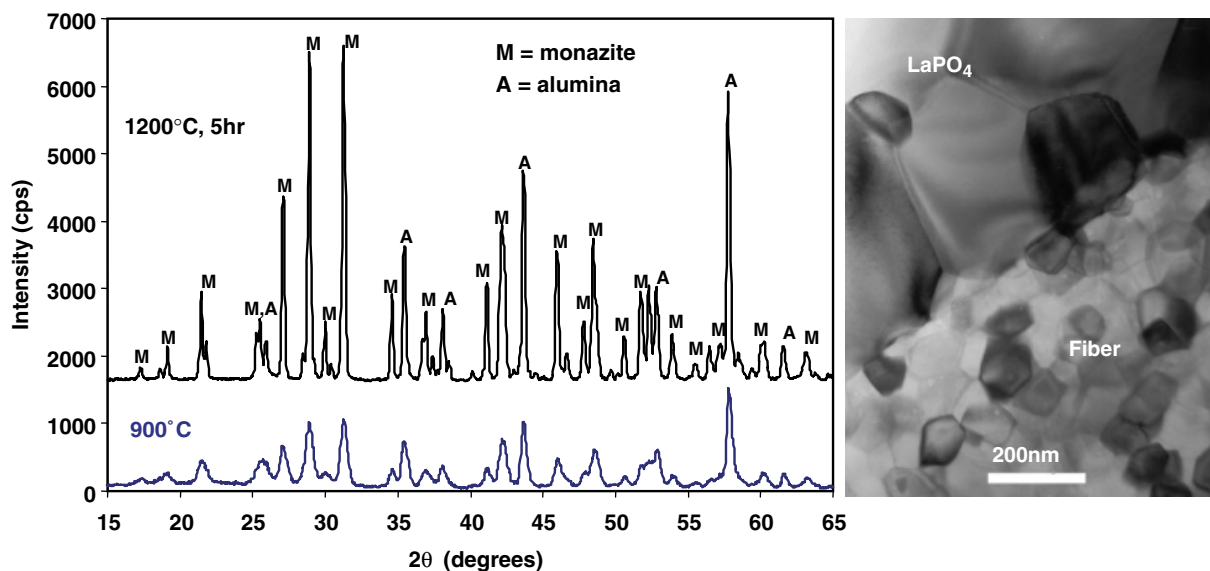**Fig. 2.** X-ray diffraction patterns of coatings (5 × 4.7 g monazite/L) in both the as-processed condition as well as after heating to 1200°C for 5 h. Transmission electron microscopy micrographs of the monazite coatings on Nextel 610 fibers (5 × 4.7 g monazite/L). La:citrate = 1:5.
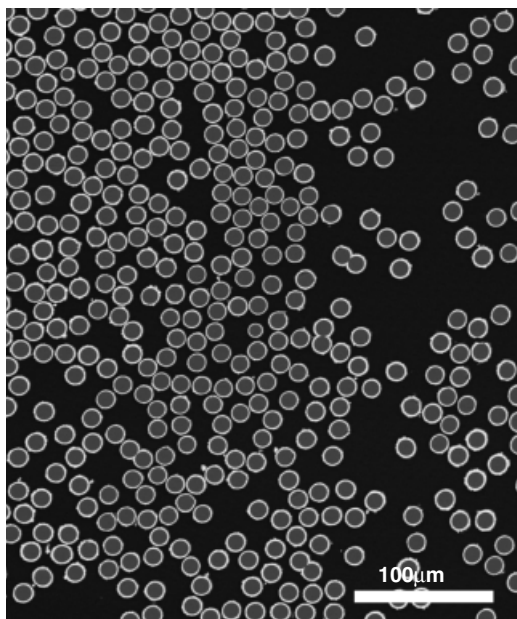
Fig. 3. Backscatter scanning electron microscope micrographs of polished cross-sections of loose tows coated five times with precursor solution yielding 3 g monazite/L. La:citrate = 1:5.

Fig. 5. Effect of both the solids loading of the precursor solution and fiber loading on the observed precipitation coating process.

for greater separations, the coating thickness is independent of separation distance. It should be noted that the image analysis yields the average coating thickness of individual fibers in the micrographs; reported coating thicknesses of < 50 nm (near the resolution limit of the technique) arise when the fiber has a small, resolvable patch of coating that is then averaged over the fiber surface.[21]
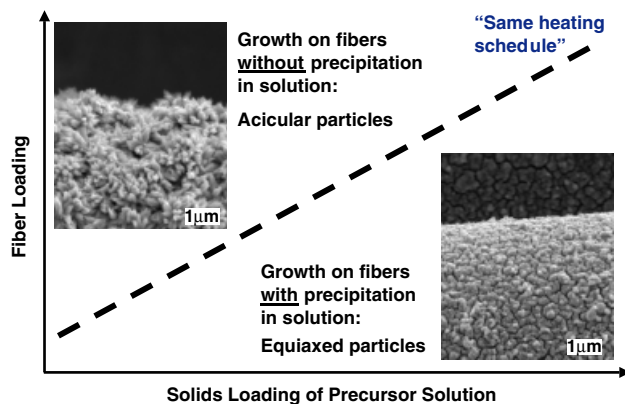
(2) Revised Cloth-Coating Procedure

Figure 8 schematically illustrates the experimental setup of process B and shows backscatter SEM micrographs of polished cross-sections of cloths coated 14 times with precursor solution yielding 100 g LaPO$_4$/L. The coatings are shown to be of similar thickness but more uniform than those applied using process A in regions of both loose and tight fiber packing. SEM examination of the surfaces of the coated fibers revealed an equiaxed coating particle morphology. Fibers extracted from the cloth coated 14 times had an average strength of 2.02 ± 0.22 GPa in the as-processed state; following a 2-h heat treatment at 1200°C in air, the average fiber strength declined to ~ 1 GPa.

Figure 9 shows the results of the coating thickness analysis of the SEM micrographs of polished cross sections of cloths coated 14 times with precursor solution yielding 100 g LaPO$_4$/L using process B. The average coating thickness of each fiber in the micrographs is plotted as a function of the average fiber separation calculated as described above. The coating thickness of a
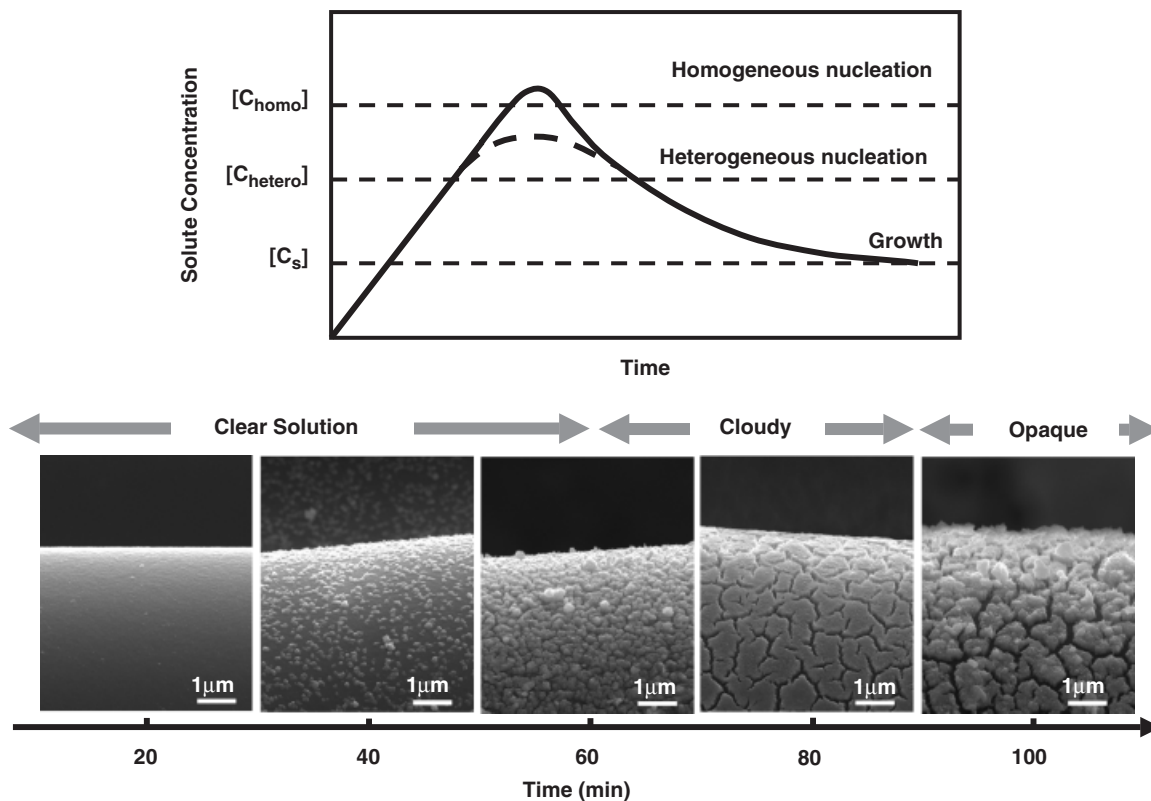

Fig. 4. Modified LaMer diagram and evolution of the coating on the fiber surface during a single coating step as a function of time at a constant temperature of 20°C and solids yield of 3 g monazite/L. La:citrate = 1:5.
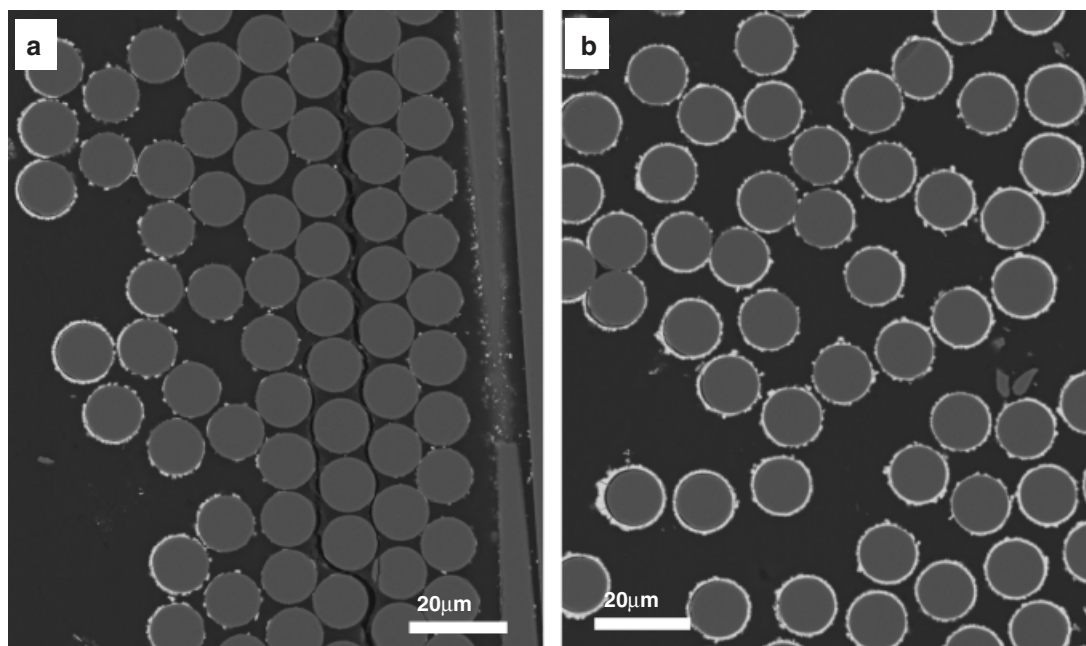
Fig. 6. Backscatter scanning electron microscope micrographs of polished cross-sections of cloths coated six times with precursor solution yielding 1 g monazite/L. La:citrate = 1:5. (a) tightly packed region and (b) loosely packed region.

particular fiber is directly proportional to the fiber separation as well as the volume of solution closest to that fiber.

IV. Discussion

(1) Initial Cloth and Tow Coating Experiments (Process A)

When the precursor solution concentration was high and the fiber loading was low (Fig. 5), hydrated $LaPO_4$ precipitated both on the fiber surface and in solution. In these cases, thick coatings were obtained, which formed a crust bridging several fibers within the tows together. The crust was limited to portions of the fiber tows easily accessed by the solution, i.e., the loosely packed regions of the cloth and the perimeter of the tightly packed tows. Under these conditions, coatings are comprised of both particles that nucleated on the fiber surface and particles that nucleated homogeneously in the solution and adhered to the fiber surface, leading to a fluffy appearance in cross section. When fiber tows are coated in place of cloths, highly uniform coatings are obtained with no crust formation and minimal fiber bridging; presumably, this is due to the lack of constraint of the fibers, allowing them to flow freely during the coating process, in contrast to fibers within the woven cloth.

Further evidence of the heterogeneous nucleation in this regime is provided in Fig. 4 and can be explained using the modified LaMer diagram.[25] Under these conditions, the coating nucleates heterogeneously on the fiber surface while the solution remains clear, indicating a lack of homogeneous nucleation. The fiber surface provides low energy nucleation sites for the coating at solute concentrations below C_{homo} (Fig. 4). With time, the solution becomes cloudy and then opaque as particles nucleate homogeneously at solute concentrations above C_{homo}; at the same time the coatings on the fibers roughen substantially as agglomerates nucleate homogeneously in solution adhere to them. In contrast, when the precursor solution concentration was low and the fiber loading was high, $LaPO_4 \cdot nH_2O$ did not precipitate in the bulk solution; precursor solutions containing cloths and fiber tows were heated to precipitate $LaPO_4 \cdot nH_2O$ but remained clear. Upon removal from the heated solutions, the fibers were coated. In these cases, the concentration of solute in solution remained below that needed for homogeneous nucleation (below C_{homo}) and the coatings were thinner than in cases where precipitation in solution occurred.

In both coating regimes, coatings were either extremely thin, discontinuous, or absent in regions of tight fiber packing (tow cross overs). For cases in which precipitation of the $LaPO_4 \cdot nH_2O$ occurred both in solution and on the fiber surface, a lack of coating in the tightly packed regions may be expected if the coating bridges fibers and seals off these areas; in this case the coating would only be derived from the small volume of precursor in the immediate vicinity of the fiber. In contrast, when $LaPO_4 \cdot nH_2O$ does not precipitate in solution, precipitation of the coating on the fiber surface must occur by transport of the reactants (lanthanum citrate and phosphoric acid) to the surface where they react to form coating particles, similar to a CVD coating process. Uniform deposition of solids by CVD on planar substrates and fiber preforms has been shown to be highly dependent on the relative rates of reactant transport and chemical reaction at the surface.[26–29] Non-uniform deposition arises when the rate of reaction greatly exceeds the rate of transport; this effect is magnified by the tortuous diffusion routes present in fiber preforms but can be alleviated by assisting reactant transport via convection, etc.
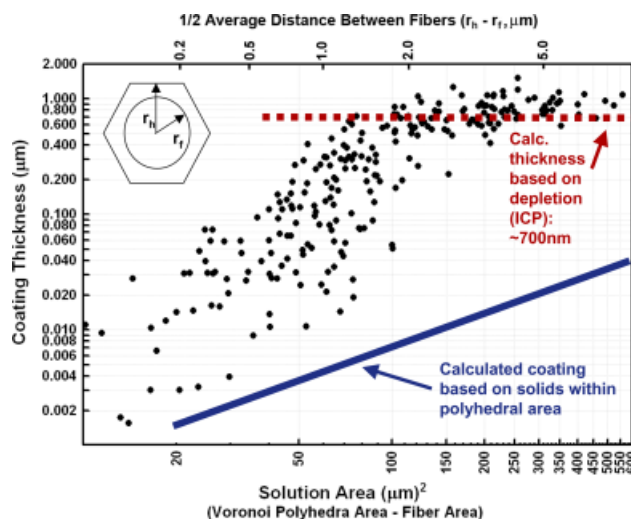

Fig. 7. Results of the coating thickness analysis of scanning electron microscope micrographs of polished cross-sections of cloths coated six times with precursor solution yielding 1 g monazite/L. La:citrate = 1:5.

Process B: Saturate and submerge in warm water
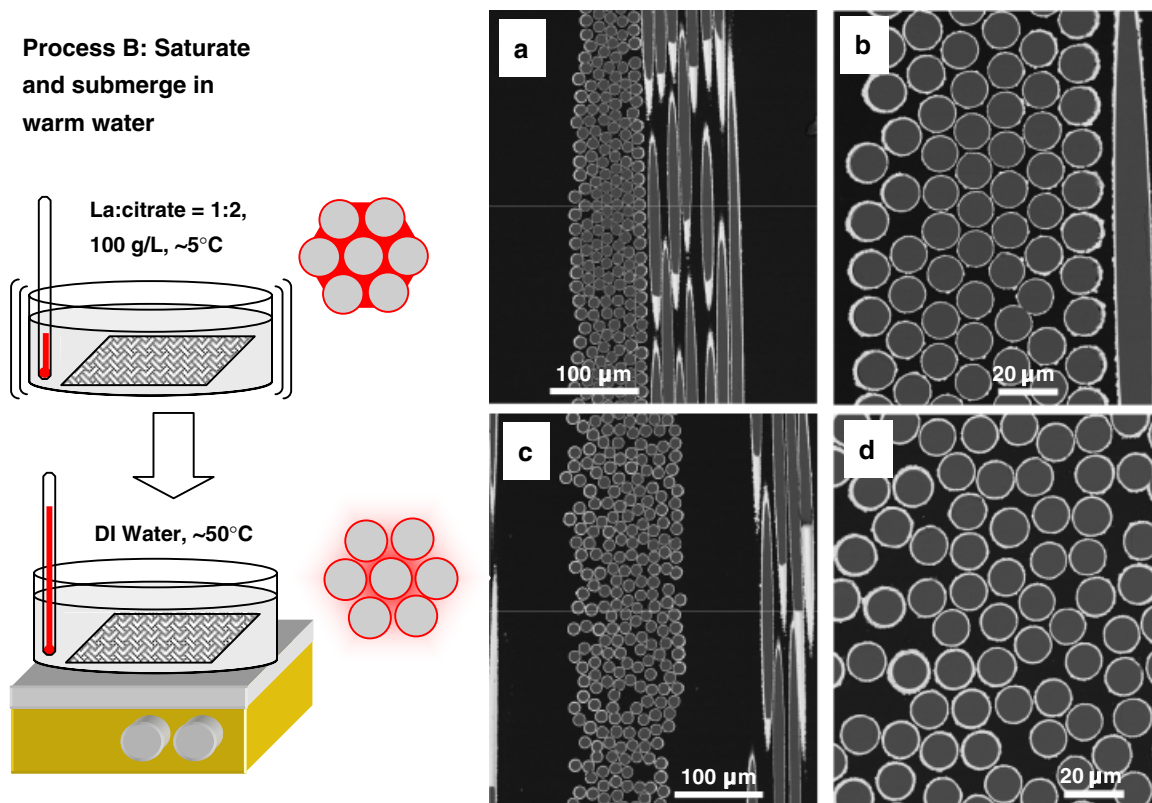
La:citrate = 1:2, 100 g/L, ~5°C

DI Water, ~50°C

Fig. 8. Schematic of experimental set up of process B and backscatter scanning electron microscope micrographs of polished cross-sections of cloths coated 14 times with precursor solution yielding 100 g monazite/L. La:citrate = 1:2. (a) and (b) tightly packed region. (c) and (d) loosely packed region.

Uniform deposition of coatings when there is no precipitation in solution is similarly expected to be dependent on the relative rates of mass transport and reaction. As the reactant concentration in the vicinity of the fiber surface becomes locally depleted (*radially* from the fiber axis), it must be replenished by mass transport of additional reactant species from the bulk solution. Assuming a constant surface reaction rate, the time necessary to deplete the reactants increases with increasing fiber separation. Reactant transport to depleted regions may occur in both radial and axial directions; however, for the case of tightly packed fibers (perfect hexagonal packing), transport in the axial direction is expected to dominate. If the rate of reaction at the fiber surface is much greater than the rate of transport of reactants to the surface, it is highly probable that reactants in transit from the bulk solution encounter another fiber surface or other growing nuclei to react with before reaching the interior of the tightly packed regions; consequently, very little coating would be deposited in the regions of tightly packed fibers and the majority of deposition would occur in loosely packed regions to which reactant species have freer access.

Image analysis of SEM micrographs[21] of cloths coated under conditions in which no precipitation occurs in solution shows a strong correlation between fiber separation and average coating thickness (Fig. 7). Also shown in Fig. 7 is the expected average coating thickness (assuming relative density = 0.6) based on 1) the depletion of the reactants from the solution as determined by inductive coupled plasma optical emission spectroscopy (ICP-OES) and (2) the known precursor solution concentration and fiber loading. The coating thicknesses are near the expected value for average fiber separations above ~3 μm. The fact that the coating thickness is independent of fiber separation beyond 3 μm may be attributed to convective mass transport caused by stirring the precursor solution during coating deposition; this effect is similarly realized in the case of loose fiber tows resulting in highly uniform coatings (Fig. 3). At separations below ~3 μm, the measured coating thickness lies below the expected value and decreases linearly with decreasing fiber separation. Figure 7 also shows the predicted coating thickness assuming that the coating is only due to the small solution volume around individual fibers for each coat (six total coats at 1 g/L). The fact that the measured coatings lie well above this prediction for almost all fiber separations indicates that transport of reactants from the bulk solution into the woven fibers is occurring; however, as fibers become very tightly packed (small separations) the measured coatings approach the predicted values, indicating that reactants from the bulk solution do not reach these fibers. These results suggest that coating deposition in the regions of tight fiber packing is limited by the rate of transport of reactants from the bulk solution.

The lack of coating in tightly packed fibers for cases in which no precipitation occurs in solution can be modeled using the approaches derived for catalysis in porous media and chemical
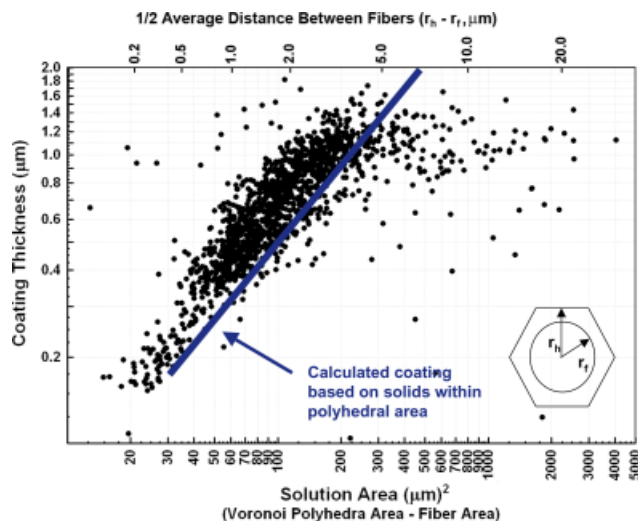

Fig. 9. Results of the coating thickness analysis of the scanning electron microscope micrographs of polished cross-sections of cloths coated 14 times with precursor solution yielding 100 g monazite/L using Process B. La:citrate = 1:2.

vapor infiltration (CVI) of fiber preforms.[27–29] These models treat the fiber preform as an array of pores into which reactants diffuse and subsequently react to yield a solid. Assuming the chemical reaction to be first-order, the diffusion equation to be solved is:

$$\frac{d^2C}{dz^2} = \frac{kS}{D}C \tag{1}$$

where k is the first order reaction constant, S is the surface area of the perform, and D is the diffusion coefficient of the reactants. The relevant boundary conditions are ($z = 0$ at the center of the preform)

$$C(z = L) = C_0$$
$$\frac{dC}{dz}(z = 0) = 0 \tag{2}$$

where C_0 is the reactant concentration outside of the preform. For deposition from both sides of a plate of thickness 2L with pores of radius R, the solution of Eq. (1) subject to the boundary conditions gives the reactant concentration along the length of the pores as

$$\frac{C(z)}{C_0} = \frac{\cos h\left(z\sqrt{2k/RD}\right)}{\cos h\left(L\sqrt{2k/RD}\right)} \tag{3}$$

To model coating deposition in tightly packed fibers, the plate thickness 2L in the model is set equal to the length of the tightly packed regions along the tows comprising the cloth (~ 800 μm); the voids between tightly packed fibers are modeled as a hexagonal array of circular pores of radius $R = 1$ μm. Transport into the pores occurs along the axial direction of the fibers.

For precipitation from solution, the diffusion coefficient D in Eq. (3) is assumed to be given by the Einstein relationship

$$D(T) = \frac{k_b T}{6\pi \eta r} (m^2/s) \tag{4}$$

where k_b is Boltzmann's constant, T is temperature, η is the (temperature dependent) viscosity of the solution, and r is the radius of the diffusing species (4.5 Å for La^{3+}).[30] The reaction constant k can be estimated knowing the time to react a fixed amount of solution precursors at various temperatures and assuming that the temperature dependence follows an Arrhenius relation; further assume that the precursor completely precipitates onto a fixed volume of fibers comparable with that used for an actual coating experiment (for 10 g cloth, surface area ~ 1 m²). Using the data from the Results section, the reaction constant k is estimated to be

$$k = 1.4 \times 10^{12} e^{-13100/T} (m/s) \tag{5}$$

Substituting Eqs. (4) and (5) back into Eq. (3) allows the reactant concentration along the pores to be determined.

Figure 10 shows the calculated reactant concentration along the axial direction of voids between fibers in the tightly packed region at various precipitation temperatures. At all temperatures, the reactant concentration is much lower in the center of the pores than outside. Higher temperatures increase the reaction rate, leading to more deposition at the mouths of the pores. The observed coating thickness will be proportional to the calculated reactant concentration; consequently, higher temperatures are expected to lead to minimal coating deposition in the region of tightly packed fibers as observed experimentally. The analysis suggests that to obtain uniform coatings in the tightly packed fibers, the deposition must occur at a low temperature and at a slower rate. The reaction rate of the lanthanum citrate and phosphoric acid in solution can be decreased by using a higher citrate concentration; however, as with commercial CVD/CVI processes, lower deposition rates lead to long processing times. During most coating experiments, the temperature
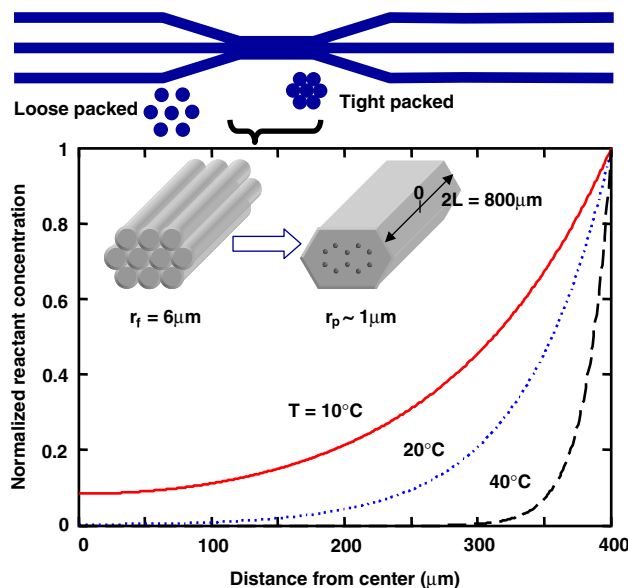

Fig. 10. Normalized reactant concentration along length of pores in region of tight fiber packing as a function of precipitation temperature with precursor concentration = 3 g monazite/L assuming no precipitation in solution.

of the precursor solution was raised from 5 to $\sim 35°$C over a period of 80 min with constant stirring. In light of the analysis above, very little coating deposition is expected in the tightly packed regions under these conditions. The stirring of the solution may assist transport of reactants to the tightly packed regions as in CVI under force-flow conditions and is not accounted for in the analysis.[27]

(2) Revised Cloth Coating Procedure (Process B)

The results to this point have shown that while $LaPO_4 \cdot nH_2O$ is precipitated onto loosely packed fibers, the deposition into the interior of the tightly packed regions of the cloth is limited by transport of the reactants to these areas; calculations have shown that lower precipitation temperatures may improve coating uniformity but only at the expense of short processing times. As a potential solution to this problem, a revised coating process (Process B) was adopted in which the concentration gradient of the precursor solution is reversed and the reaction to precipitate $LaPO_4 \cdot nH_2O$ is made to occur rapidly. The coating precipitates within several seconds at a water temperature of 50°C; the rapid precipitation is due to the temperature of the water (faster reaction kinetics at higher temperatures). The reaction rate may also be increased by reducing the amount of citrate used to chelate the lanthanum ions.

As shown in Fig. 8, the coatings from process B are quite uniform in both the tightly packed and loosely packed regions of the cloth; bridging of fibers by coating is not observed. The coating uniformity is a consequence of having a large amount of reactants in the immediate vicinity of the fiber surfaces including the tightly packed regions. There still exists a gradient in coating thickness between the interior fibers of the tightly packed region and those on the exterior; this is due to the limited diffusion of the precursor solution out of these regions upon submersion in warm water leading to slightly greater deposition on the exterior of the tows. Further analysis of the coating uniformity via image analysis reveals that the coating thickness of an individual fiber is directly proportional the area of solution in its immediate vicinity as shown in Fig. 9. Larger solution area (more precursor in fiber vicinity) leads to thicker coatings. These results also imply that the coating thickness distribution in the coated cloth is derived from the fiber separation distribution; woven articles that have a more narrow distribution of fiber separation will

consequently have a more narrow coating thickness distribution when coated using process B.

The average fiber strength in this case ($\sim$2 GPa) was lower than that observed for fibers from tows extracted from desized, uncoated Nextel™ 610 cloths (2.6–2.8 GPa). The lower strength indicates that the fibers have been affected in some way by the coating process and severely affected by the 2 h exposure at 1200°C. The observed fiber strength degradation is not entirely unexpected; fiber strength degradation of LaPO$_4$-coated fibers has been observed by Boakye *et al.*[24,31] and has been attributed to a stress–corrosion process in which the fiber is attacked at high-temperature by the decomposition products of the solution-derived coating. Efforts to improve the strength of fibers coated using process B discussed herein will be described in a companion paper.

V.   Conclusion

A process for coating woven ceramic fibers with LaPO$_4$ has been demonstrated wherein the coatings are applied using solution precursors via heterogeneous nucleation and growth on the fiber surface. The temperature dependence of the rate of reaction between lanthanum citrate and phosphoric acid in solution may be exploited to coat woven articles of ceramic fibers by (1) mixing coating precursor solutions at low-temperature where the reaction is extremely sluggish, (2) saturating the woven ceramic fibers in this mixed solution and, (3) submerging the saturated cloth in warm water to affect rapid precipitation. As the reaction proceeds, the coating nucleates and grows on the fiber surfaces. Under appropriate conditions, high-quality coatings are obtained with excellent coating coverage in the areas of tightly packed fibers. The process requires only very straightforward equipment and is compatible with existing CMC processes. Current work is focused on optimizing the process by varying the chemistry with the goal of retaining the strength of the coated fibers following heat treatment at the matrix processing temperature.

References

[1]A. G. Evans and D. B. Marshall, "The Mechanical Behavior of Ceramic Matrix Composites," *Acta. Metall.*, **37** [10] 2567–83 (1989).

[2]A. G. Evans and F. W. Zok, "The Physics and Mechanics of Fiber-Reinforced Brittle Matrix Composites," *J. Mater. Sci.*, **29**, 3857–96 (1994).

[3]A. G. Evans, F. W. Zok, and J. B. Davis, "The Role of Interfaces in Fiber-Reinforced Brittle Matrix Composites," *Compos. Sci. Technol.*, **42**, 3–24 (1991).

[4]R. J. Kerans, R. S. Hay, N. J. Pagano, and T. A. Parthasarathy, "The Role of the Fiber–Matrix Interface in Ceramic Composites," *Am. Ceram. Soc. Bull.*, **68** [2] 429–42 (1989).

[5]L. Filipuzzi, G. Camus, and R. Naslain, "Oxidation Mechanisms and Kinetics of 1D-SiC/C/SiC Composite Materials: I, An Experimental Approach," *J. Am. Ceram. Soc.*, **77** [2] 459–66 (1994).

[6]G. N. Morscher and J. D. Cawley, "Intermediate Temperature Strength Degradation in SiC/SiC Composites," *J. Eur. Ceram. Soc.*, **22**, 2777–87 (2002).

[7]P. E. D. Morgan and D. B. Marshall, "Functional Interfaces for Oxide/Oxide Composites," *Mater. Sci. Eng.*, **A126**, 15–26 (1993).

[8]R. J. Kerans, R. S. Hay, T. A. Parthasarathy, and M. K. Cinibulk, "Interface Design for Oxidation-Resistant Ceramic Composites," *J. Am. Ceram. Soc.*, **85** [11] 2599–632 (2002).

[9]K. A. Keller, T. Mah, T. A. Parthasarathy, E. E. Boakye, P. Mogilevsky, and M. K. Cinibulk, "Effectiveness of Monazite Coatings in Oxide/Oxide Composites after Long-Term Exposure at High Temperature," *J. Am. Ceram. Soc.*, **86** [2] 325–32 (2003).

[10]T. J. Hwang, M. R. Hendrick, H. Shao, H. G. Hornis, and A. T. Hunt, "Combustion Chemical Vapor Deposition (CCVD) of LaPO$_4$ Monazite and Beta-alumina on Alumina Fibers for Ceramic Matrix Composites," *Mater. Sci. Eng.*, **A244**, 91–6 (1998).

[11]R. S. Hay "Method for Coating Continuous Tows," U. S. Pat. No. 5,164,229, 17, 1992.

[12]E. Boakye, R. S. Hay, and M. D. Petry, "Continuous Coating of Oxide Fiber Tows using Liquid Precursors: Monazite Coatings on Nextel 720," *J. Am. Ceram. Soc.*, **82** [9] 2321–31 (1999).

[13]M. K. Cinibulk, "Sol–Gel Coating of Nicalon™ Fiber Cloths," *Ceram. Eng. Sci. Proc.*, **17** [4] 241–9 (1996).

[14]M. K. Cinibulk, "Deposition of Oxide Coatings on Fiber Cloths by Electrostatic Attraction," *J. Am. Ceram. Soc.*, **80** [2] 453–60 (1997).

[15]A. R. Boccaccini, P. Karapappas, J. M. Marijuan, and C. Kaya, "TiO$_2$ Coatings on Silicon Carbide Fiber Substrates by Electrophoretic Deposition," *J. Mater. Sci.*, **39** [1] 851–9 (2004).

[16]E. E. Boakye, T. Mah, C. M. Cooke, K. Keller, and R. J. Kerans, "Initial Assessment of the Weavability of Monazite-Coated Oxide Fibers," *J. Am. Ceram. Soc.*, **87** [9] 1775–8 (2004).

[17]T. Yano, P. Lee, and M. Imai, "In-situ Reaction Deposition Coating of LaPO$_4$ on Al$_2$O$_3$ Fabric Cloth for Al$_2$O$_3$/Al$_2$O$_3$ Composites," *Ceram. Sci. Eng. Proc.*, **25** [4] 93–8 (2004).

[18]E. E. Boakye, P. Mogilevsky, and R. S. Hay, "Synthesis of Nanosized Spherical Rhabdophane Particles," *J. Am. Ceram. Soc.*, **88** [10] 2740–6 (2005).

[19]M. K. Cinibulk, J. R. Welch, and R. S. Hay, "Preparation of Thin Sections of Coated Fibers for Characterization by Transmission Electron Microscopy," *J. Am. Ceram. Soc.*, **79** [9] 2481–4 (1996).

[20]M. K. Cinibulk, J. R. Welch, and R. S. Hay, "Transmission Electron Microscopy Specimen Preparation of Ceramic Coatings on Ceramic Fibers," *Mater. Res. Soc. Symp. Proc.*, **480**, 3–17 (1997).

[21]R. S. Hay, G. Fair, P. Mogilevsky, and E. Boakye, "Measurement of Fiber Coating Thickness Variation," *Ceram. Sci. Eng. Proc.*, **26** [2] 11–8 (2005).

[22]M. D. Petry, T. Mah, and R. J. Kerans, "Validity of Using Average Diameter for Determination of Tensile Strength and Weibull Modulus of Ceramic Filaments," *J. Am. Ceram. Soc.*, **80** [10] 2741–4 (1997).

[23]M. D. Petry and T.-I. Mah, "Effect of Thermal Exposures on the Strength of Nextel 550 and 720 Filaments," *J. Am. Ceram. Soc.*, **82** [10] 2801–7 (1999).

[24]E. E. Boakye, R. S. Hay, P. Mogilevsky, and L. M. Douglas, "Monazite Coatings on Fibers: I, Effect of Temperature and Alumina Doping on Coated-Fiber Strength," *J. Am. Ceram. Soc.*, **84** [12] 2783–92 (2001).

[25]A. K. Garg and L. C. DeJonghe, "Microencapsulation of Silicon Nitride Particles with Yttria and Yttria–Alumina Precursors," *J. Mater. Res.*, **5** [1] 136–42 (1990).

[26]A. Yeckel, S. Middleman, and A. K. Hochberg, "The Origin of Nonuniform Growth of LPCVD Films from Silane Gas Mixtures," *J. Electrochem. Soc.*, **136** [7] 2038–50 (1989).

[27]W. J. Lackey and T. L. Starr, "Fabrication of Fiber-reinforced Ceramic Composites by Chemical Vapor Infiltration: Processing, Structure, and Properties"; pp. 397–450 in *Fiber Reinforced Ceramic Composites*, Edited by K. S. Mazdiyasni. Noyes, Park Ridge, NJ, 1990.

[28]E. O. Einset, N. Patibandla, and K. L. Luthra, "Processing Conditions for Boron Nitride Coatings in Fiber Bundles Via Chemical Vapor Deposition," *J. Am. Ceram. Soc.*, **77** [12] 3081–6 (1994).

[29]S. K. Griffiths and R. H. Nilson, "Optimum Conditions for Composites Fiber Coating by Chemical Vapor Infiltration," *J. Electrochem. Soc.*, **145** [4] 1263–72 (1998).

[30]J. Kielland, "Individual Activity Coefficients of Ions in Aqueous Solutions," *J. Am. Chem. Soc.*, **59**, 1675–8 (1937).

[31]E. E. Boakye, R. S. Hay, P. Mogilevsky, and L. M. Douglas, "Monazite Coatings on Fibers: II, Coating without Strength Degradation," *J. Am. Ceram. Soc.*, **84** [12] 2793–801 (2001).   □